



Performance indicators for portable X-ray fluorescence devices

Eleni Konstantakopoulou¹, Annalaura Casanova Municchia², Roberto Ferretti³, Simone Porcinai⁴, Marco Ferretti²

¹ Polytechnic School, Aristotle University of Thessaloniki, University Campus, 54124 Thessaloniki, Greece

² Institute of Heritage Science (CNR-ISPC), National Research Council of Italy, Area della Ricerca di Roma 1, Montelibretti, Via Salaria Km 29,300, 00010 Rome, Italy

³ Department of Mathematics and Physics, Roma Tre University, Largo San Leonardo Murialdo 1, 00146 Rome, Italy

⁴ Ministry of Culture – Opificio delle Pietre Dure, viale F. Strozzi, 1 – 50129 Florence, Italy

ABSTRACT

The invention of hand-held X-ray fluorescence devices (HH-XRF) has revolutionized the way we analyse ancient materials. These devices are equipped with highly miniaturized hardware and advanced software, which encourages users to consider them as black boxes. This enables archaeologists, art historians, and restorers to be self-sufficient in performing materials analysis. However, there are specific situations, such as the investigation of copper-based artefacts, where users need to have a deeper understanding of the device's functioning. This article discusses the experiments carried out to reconfigure a hand-held Bruker Tracer 5g from scratch, compare it with an in-house developed portable spectrometer, and prepare both devices for field use. We focus on optimizing the primary filters and calibrating the devices by considering two quantitative parameters: the limit of quantification and the relative uncertainty of quantification.

Section: RESEARCH PAPER

Keywords: Copper alloy; hand-held X-ray fluorescence; limit of quantification; calibration

Citation: E. Konstantakopoulou, A. Casanova Municchia, R. Ferretti, S. Porcinai, M. Ferretti, Performance indicators for portable X-ray fluorescence devices, Acta IMEKO, vol. 14 (2025) no. 1, pp. 1-6. DOI: [10.21014/actaimeko.v14i1.1864](https://doi.org/10.21014/actaimeko.v14i1.1864)

Section Editor: Fabio Leccese, Università Degli Studi Roma Tre, Rome, Italy

Received April 8, 2024; **In final form** December 10, 2024; **Published** March 2025

Copyright: This is an open-access article distributed under the terms of the Creative Commons Attribution 3.0 License, which permits unrestricted use, distribution, and reproduction in any medium, provided the original author and source are credited.

Corresponding author: Annalaura Casanova Municchia, e-mail: annalaura.casanovamunicchia@cnr.it

1. INTRODUCTION

X-ray fluorescence (XRF) has been used to analyse ancient materials for a long time, with the first articles dating back 65 years ago [1]. Portable XRF systems have been utilised for at least 50 years [2], [3]. However, only in recent times has the cultural approach towards the technique changed significantly. Operation of the instruments and interpretation of data are no longer the exclusive domain of users with natural sciences background. This change occurred with the introduction of hand-held XRF devices (HH-XRF), which have become widely used [4]. These devices (shown in Figure 1 right) have a gun-like shape and are completely self-contained. They are battery-powered, automatically controlled by an on-board computer, and can provide the results of the analysis without requiring external connections or off-line data processing. Their user-friendly design makes it seem like using XRF technology is as easy as taking aim and shooting. This has helped archaeologists, art

historians, and restorers to become self-sufficient in analysing materials and interpreting data.

It is not within the scope of this paper to discuss whether this approach is always beneficial for gaining a deeper understanding of ancient materials. Instead, it aims at discussing how suitable the general-purpose configuration of a HH-XRF device provided by the manufacturer is for the specific purpose of analysing ancient copper-based alloys. It will become evident in the following that considering the device as a black box is not sufficient anymore and that its configuration and correct use requires a comprehensive understanding of the working principles of the spectrometer.

To understand the specific requirements put by the analysis of ancient copper-based alloys, one should consider that not only the main alloying elements – i.e. Cu, Zn, Sn, and Pb – but also the minor ones – typically Co, Ni, As, Ag, Sb and Bi – are significant and need to be investigated [5]. Given the excitation



Figure 1. The XRF devices used for the experiments: F-70 (left) and Bruker Tracer 5g (right).

conditions of a portable device, most elements are quantified by either K- or L-lines solely. The only exception are medium-Z elements (i.e. Ag, Cd, Sn and Sb), for which both L- and K-lines can in principle be used. The L-lines, however, interfere with one another, so that the use of the K-lines becomes almost inevitable. Moreover, due to their relatively high energy, the latter are less affected by corrosion. This explains why, in the design of F-70 (see below), we considered efficient excitation of the K-lines of Ag, Cd, Sn and Sb so important. In particular, we opted for an X-ray tube working at 70 kV, a much higher voltage than that used by commercial HH-XRFs and for filters preferentially tailored on those elements.

We used two devices: a hand-held Bruker Tracer 5g and a portable spectrometer identified as F-70. The latter was expressly designed for the analysis of copper-based alloys and serves as a basis of comparison. The paper discusses the experiments conducted to prepare the instruments for field use, by focusing on two crucial issues, i.e. filtration of the primary beam and calibration of the device, and by considering two parameters: the limit of quantification (LOQ) and the relative uncertainty of quantification (RUOQ).

The tests were carried out trying to reproduce the working conditions and parameters that the designer assumed for field use. It is obvious that, due to the radically different design, they may change from one device to the other.

2. MATERIALS AND METHODS

2.1. Instruments

Two portable XRF spectrometers – a Bruker Tracer 5g and the in-house designed F-70 (Figure 1) – were tuned and tested in a comparative way. As discussed in the previous section, the experimental conditions try to reproduce those of field investigation of copper-based artefacts. They include operating the X-ray tubes at the maximum allowed voltage to provide the best possible excitation of the K-lines of Ag, Cd, Sn and Sb, a beam size not larger than 3 mm and a dead time not exceeding 20 %.

Measuring time deserves a detailed discussion. Much of the highly innovative character of HH-XRFs relies exactly on that (HH) that is, they are designed to be supported by the operator's arm. The price to pay is that the measuring time must be short, consistently with operator's ability to stay still. Conversely, F-70, whose architecture is more conventional, is mechanically supported, which allows for measuring times as long as the user requires. Believing that short measuring times are intrinsic to the design of Tracer, we used different values for the two devices, i.e. 30 s for Tracer 5g and 100 s for F-70. Whenever possible, to allow for a more complete comparison of the time-dependent

Table 1. Bruker Tracer 5g and F-70 working conditions and parameters, including the filters.

Device	Source	Collimator	Filters
Bruker Tracer 5g	Rh anode $HV = 49 \text{ kV}$ $i = 39.31 \text{ }\mu\text{A}$	3 mm	Ti 25 μm + Al 300 μm ; Cu 75 μm + Ti 25 μm + Al 200 μm
	Rh anode $HV = 40 \text{ kV}$ $i = 100 \text{ }\mu\text{A}$		Cu 48 μm ; Cu 72 μm ; Cu 72 μm + Al 150 μm ; Cu 100 μm ; Cu 200 μm ; Cu 200 μm + CrFeNi 35 μm ; Zn 450 μm
F-70	W anode $HV = 70 \text{ kV}$ $i = 55 \text{ }\mu\text{A}$	2 mm	

figures – the LOQs, see below – we will provide an estimate of the values that would result, should the measuring time be the same for both devices.

Being an in-house developed device, the F-70 is flexible and allows for a number of options regarding both collimators and filters. Conversely, Tracer 5g is only equipped with two collimators, i.e. 3 mm and 8 mm, and four combinations of filters. Moreover, Tracer 5g has a maximum high voltage of 50 kV, while the F-70 can operate at 70 kV. To reduce power consumption and avoid overloads, the Tracer 5g has automatic limitations on the tube current depending on the voltage. A summary of the working conditions and parameters used for each device is provided in Table 1.

2.2. Reference materials

Twenty-six certified reference materials (CRMs), compositionally significant of heritage copper-based artefacts, were used in the experiments (see Table 2). They include (but are not limited to) CRMs from the CHARM Set [6]. The analysed elements are Mn, Fe, Co, Ni, Zn, As, Ag, Cd, Sn, Sb, Pb, and Bi. Uncertainties in the certified concentration values are in most cases below 1 wt% at 95 wt% confidence level.

2.3. Data processing

For each device, the experiments involved 10 complete series of measurements on all the standards. For each device, the data set is therefore composed of 260 records.

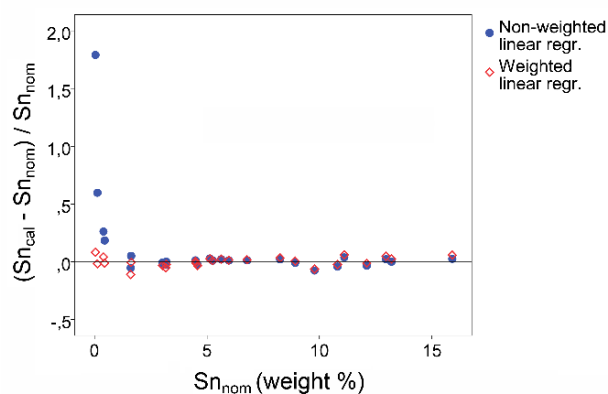


Figure 2. Scatterplot of the relative errors of calibrated Sn concentrations versus the corresponding nominal concentrations for a non-weighted (solid blue circles) and a weighted (red diamonds) linear regression.

Table 2. Supplier and composition, expressed in wt%, of the 26 CRMs.

ID	Supplier	Mg	Al	Si	P	S	Cr	Mn	Fe	Co	Ni	Cu	Zn	As	Se	Ag	Cd	Sn	Sb	Te	Au	Pb	Bi
1116	Dept. of Commerce Malcolm Baldrige Secretary (USA)				0.008				0.046		0.048	90.37	9.44				0.04					0.042	
31X 7835.8 B4		0.219		0.154				0.0102	0.045	0.313	0.157	72.7	21.55	0.151		0.549	0.094	0.451	0.110	0.101		3.22	0.101
31X 7835.9 B2		0.12	0.047	0.062	0.020			0.005	0.185	0.115	0.195	76.575	16.2	0.098	0.300	2.00	0.058	1.61	0.46			1.05	0.90
31X TB5 B6		0.071	0.111	0.025		0.0031	0.283	0.094	0.020	0.106	61.49	35.62	0.396		0.216	0.49	0.129	0.229			0.575	0.292	
32X LB10 G1				0.003	0.01				0.084	0.69	77.4	0.110	0.165		0.07		8.25	0.60	0.010		12.5	0.092	
32X LB14 G1		0.001	0.001	0.059	0.018		0.001	0.009	0.089	0.254	77.01	0.586	0.050		0.120		5.63	0.075			15.42	0.720	
32X LB17 A4	MBH Analytical LTD (UK)	0.388	0.051			0.001	0.296	0.488	0.008	0.465	74.83	0.634	1.51		0.911	0.151	5.97	4.10			9.83	0.220	
32X PB12 E3		0.033	0.007	0.007	0.172	0.013		0.011	0.032	0.014	0.221	93.29	0.546	0.087			5.25	0.160		0.102	0.057	0.033	0.007
32X SN5 B1		0.215				0.024	0.528	1.009	0.129	0.667	78.97	0.604	0.056		0.095	0.130	15.90	0.702	0.001	0.010	0.860	0.124	
32X SN6 B3		0.059				0.015	0.090	0.376	0.750	0.295	85.73	2.00	0.804		1.007	0.024	6.78	0.304		0.003	1.644	0.127	
33X GM20 B3		0.133		0.060			0.040	0.442	0.021	0.211	89.49	1.80	0.300		0.200	0.020	4.49	2.41			0.294	0.044	
33X GM21 B6		0.175	0.022	0.068	0.064			0.69		0.20	78.96	4.95	0.335	0.177	0.70	0.25	4.50	1.05			7.40	0.46	
33X GM4 AD1		0.0015	0.001	0.003	0.034		0.001	0.093	0.008	1.482	84.02	5.90	0.023		0.021		3.02	0.057			5.27	0.044	
33X RB2 A3		0.001	0.036	0.012	0.021	0.078	0.002	0.003	0.493	0.035	0.255	82.67	9.14	0.021		0.003	3.19	0.019			3.85	0.101	
B14	Centre Technique des Industries de la Fonderie (FR)			0.11	0.70	0.021		0.014	0.125		0.302	86.80	0.175	0.039				11.1	0.072			0.52	
B21	Centre de développement des industries de mise en forme (FR)		0.13		0.004	0.047			0.285		1.21	83.05	6.17					5.13	0.18			3.79	
B3	Centre Technique des Industries de la Fonderie (FR)		0.130		0.062	0.48	0.046		0.194	0.217		1.53	80.25	2.26					12.96	0.204			1.65
BS 836A-2	Brammer Standard Company (USA)	0.0015	0.002	0.083	0.042		0.001	0.025		0.46	84.7	4.55	0.008		0.023		4.58	0.068			5.32		
CURM 42.23-2	Bureau of Analysed Samples (UK)	0.008	0.008	0.015	0.128	0.045		0.019	0.354		0.168	74.36	22.13	0.168			1.63	0.356			0.575	0.034	
CURM 54.01-4			0.040	0.039	0.053	0.023		0.158	0.028		0.348	95.42	0.346	0.044			3.17	0.070			0.307		
SS551		0.052	0.018	1.01				0.20		0.76	87.4	0.74					8.92				0.79		
SS552		0.023	0.019	0.77				0.10		0.56	87.7	0.35					9.78				0.63		
SS553	British Chemical Standards (UK)	0.017	0.022	0.68				0.056		0.44	87.0	0.49					10.8				0.47		
SS555		0.005	0.036	0.18				0.010		0.11	87.1	0.16					12.1				0.24		
SS556		0.005	0.005	0.10				0.004		0.014	86.4	0.09					13.2				0.16		
UZ560	Centre de développement des industries de mise en forme (FR)		3.72	0.07					0.47		0.49	78.98	15.30					0.40				0.57	

All the spectra, including those of Tracer 5g, were off-line quantified by PyMCA, a software package based on the Fundamental Parameters method [7]. This was the only exception to the general criterion of operating each device in its field working conditions. In a previous paper, we considered Tracer 5g solely and compared several on-board and off-line calibrations and quantification methods [8]. In this work, we opted for off-line quantification.

The output of PyMCA, i.e. the measured concentrations, was then subjected to calibration. This procedure aims at making the results virtually comparable with those from other devices and/or laboratories. It consists of the linear transformation:

$$c_{\text{cal}} = a \cdot c_{\text{meas}} + b, \quad (1)$$

where: c_{cal} is the calibrated concentration; c_{meas} is the measured concentration as provided by PyMCA and a and b are the slope and the intercept of a weighted linear regression. In the regression, the measured concentrations are the independent variables and the corresponding nominal concentrations c_{nom} are the dependent ones. Only data points with c_{nom} above the limit of quantification are included, see equation (3) and Figure 6.

It is the same procedure discussed by Heginbotham et al. [9], except that ours is a weighted regression with:

$$\text{weight} = \frac{1}{c_{\text{nom}}^2}. \quad (2)$$

Applying the weights corresponds to minimising the relative deviations instead of the absolute ones. The advantage is that a weighted regression ensures that relative deviations are approximately constant all over the concentration range, whereas a non-weighted one is mainly controlled by high-concentration

values and may produce large relative errors at low concentrations. As an example, Figure 2 compares the relative errors of Sn calibrated concentrations that is, $(S_{n\text{cal}} - S_{n\text{nom}}) / S_{n\text{nom}}$. $S_{n\text{cal}}$ is calculated by a non-weighted and a weighted linear regression, respectively. It appears that the weighted regression reduces relative errors at low concentrations by approximately 10 times.

The LOQ is the minimum concentration of a given element that can be measured with a given uncertainty. If we set at $B + 10 \sigma(B)$ the limit above which the fluorescent signal is considered quantifiable [10], LOQ is calculated as follows:

$$LOQ = \frac{10 \cdot c \cdot \sqrt{B}}{P}, \quad (3)$$

where c is the concentration of the element in the sample; B is the background area, and P is the net peak area.

Strictly speaking, LOQ depends, among other variables, on the spectral interferences and is therefore unique to each sample. For the aim of this paper, however, it can be considered approximately constant. We calculated it using standards with analyte concentration of about 1 wt%. LOQ is closely linked to the excitation conditions, specifically to the spectral features of primary radiation. In this work, we use it for two purposes: a) as a figure of merit to optimize the primary beam filters, and b) to select the data points needed for calibration and for the calculation of quantification uncertainties.

Regarding the first point, it is a common practice to place absorbers on the path of the primary beam to shape the spectrum and improve the excitation conditions of the analytes of interest. They are in the form of one or more thin sheets made of one or more elements. Figure 3 and Figure 4 show the different shapes

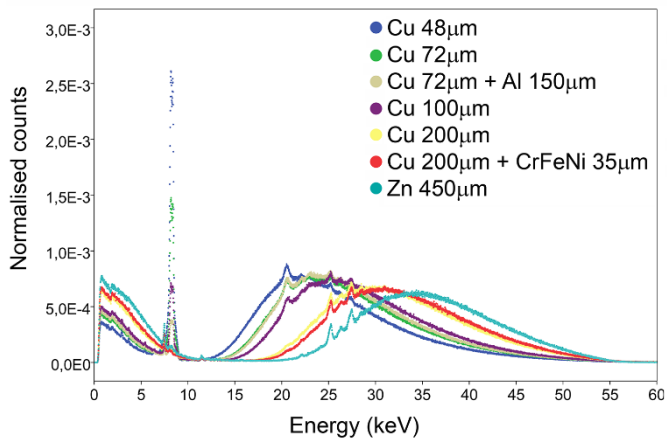


Figure 3. Comparison of the effects of different filters applied to F-70 primary beam; the spectra are normalized to 1.

taken by the primary spectra (normalized to 1) of F-70 and Bruker when different filters are applied. The spectra are acquired by placing a scatterer – i.e. a low-Z target – in front of the beam.

This method does not account for the Compton shift and introduces spectral artefacts related to scattering; however, it is simple and suitable to highlight the attenuation effects of the filter.

For a given analyte, absorbers reduce both the background under the peak and the primary intensity above its absorption edge. A suitable filter is therefore a compromise that keeps the former low and the latter high as much as possible. Further complication comes from the fact that the analytes of interest are often distributed all over the spectrum, so that a filter suitable for a given analyte may be not as suitable for all the others.

Selection of the appropriate filter is affected by too many variables to be simply approached by a visual inspection of the spectrum. We therefore propose to choose some elements (in this work they are Ni, Zn, Pb and Sn) representative of different energy ranges and to consider the corresponding LOQs. These are used to compare the performance of different filters. The best compromise should be, at least in principle, the filter that produces the lowest LOQ, averaged over the four elements.

For completeness, a high-purity copper target was measured to highlight possible differences between the blank instrumental backgrounds. The filters are those selected in section 3.1. Figure 5 overlaps the two spectra scaled to have the same copper fit area. It appears that there are no relevant differences between the backgrounds, at least in the energy ranges considered in this

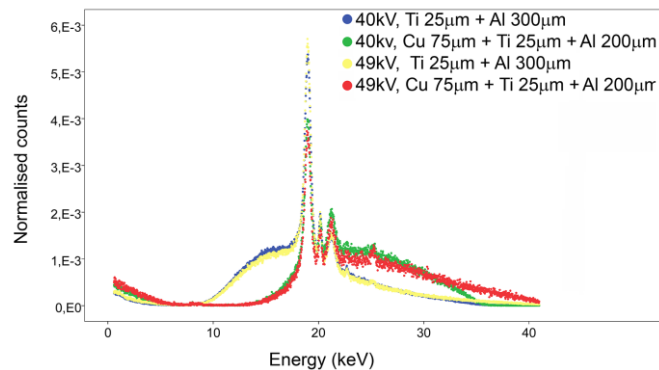


Figure 4. Comparison of the effects of different filters applied to Bruker Tracer 5g; the spectra are normalized to 1.

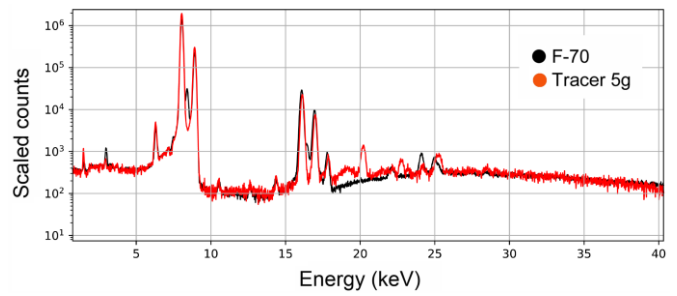


Figure 5. Comparison of high-purity copper spectra obtained by F-70 (black line) and Tracer 5g (red line); the spectra are scaled to obtain the same copper fit area.

work. Spectral contaminations, resulting from the interaction of primary/fluorescent/scattered radiation with the spectrometer materials, are present in both instruments. The most apparent ones are from Fe, Ni and Sn. Calibration ensures that they have no effect on quantification. They might however affect LOQs. By considering, at low concentration values, the intercepts of the linear regressions of nominal versus measured concentration, we concluded that contaminations can be ignored, as they affect the corresponding LOQs by less than 5 % relative.

The RUOQ is the relative uncertainty associated to the calibrated concentration. It is calculated using CRMs with $c_{nom} > LOQ$ solely and equals the standard deviation of relative residuals $(c_{cal} - c_{nom})/c_{nom}$. It will be clear in the following that it crucially depends on LOQ, as an underestimation of the latter may produce an overestimation of the former. Figure 6 summarises the meaning of the quantities discussed in this section.

3. RESULTS AND DISCUSSION

3.1. Filtration of the primary beam

The filter was optimized by calculating the LOQs of Ni, Zn, Pb, and Sn and considering the average value as a figure of merit to guide the selection. F-70 is mechanically simpler and more accessible. Fine-tuning was therefore easier than for Tracer 5g. For the latter only the filters provided by the manufacturer could be used. Moreover, one of the constraints of Tracer 5g operation is minimum battery consumption, achieved by automatically

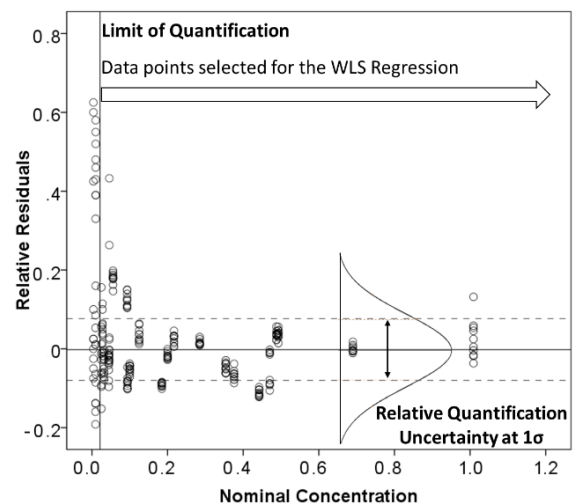


Figure 6. Synoptic graph of the quantities (LOQ and RUOQ) discussed in this section.

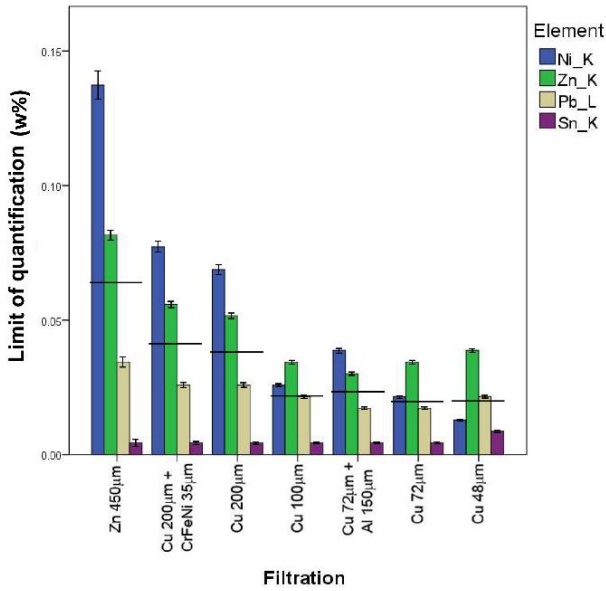


Figure 7. Optimisation of the primary filter for F-70: the bars represent the LOQs of Ni, Zn, Pb and Sn for the filters listed in the category axis; uncertainties are quoted at 2σ confidence level; the horizontal lines account for the average LOQs, used as a figure of merit to evaluate the performance of each filter.

reducing current. It will be clear in the following that such a reduction flattens the potentially attainable differences and makes filter selection somehow arbitrary. Regarding the present experiments, we tested the same filters at both 40 kV and 49 kV.

Figure 7 and Figure 8 show, for F-70 and Tracer and for the filters listed in the horizontal axis of the charts, the LOQs of Ni, Zn, Pb, and Sn, the corresponding uncertainties quoted at 2σ confidence level and the LOQ averaged over the four elements, represented by the horizontal lines. Assuming a relative uncertainty of 1 % for the nominal compositions, uncertainties of LOQs are calculated through the error propagation formula:

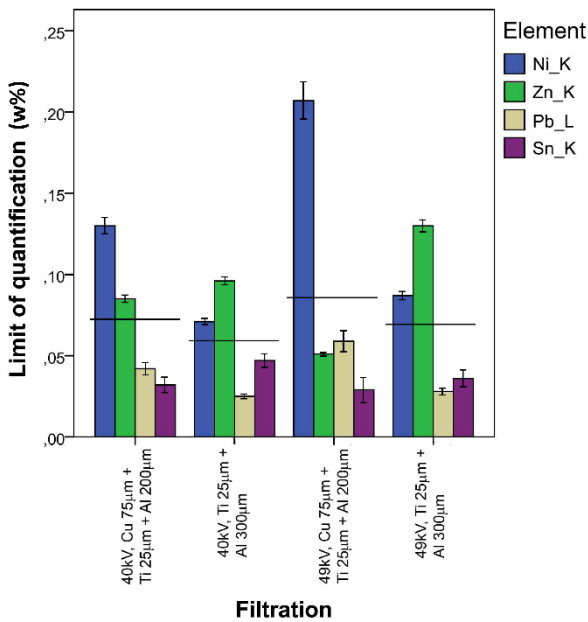


Figure 8. Optimisation of the primary filter for Tracer 5g: the bars represent the LOQs of Ni, Zn, Pb and Sn for the filters listed in the category axis; uncertainties are quoted at 2σ confidence level; the horizontal lines account for the average LOQs, used as a figure of merit to evaluate the performance of each filter.

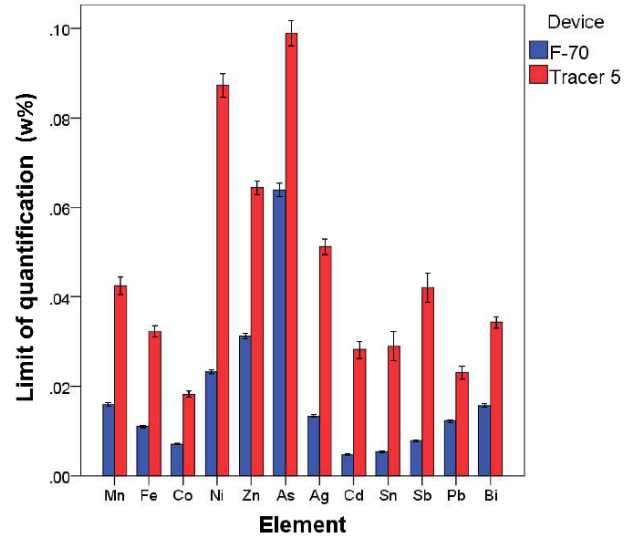


Figure 9. LOQs of the analysed elements for F-70 and Tracer 5g; uncertainties are quoted at 2σ confidence level.

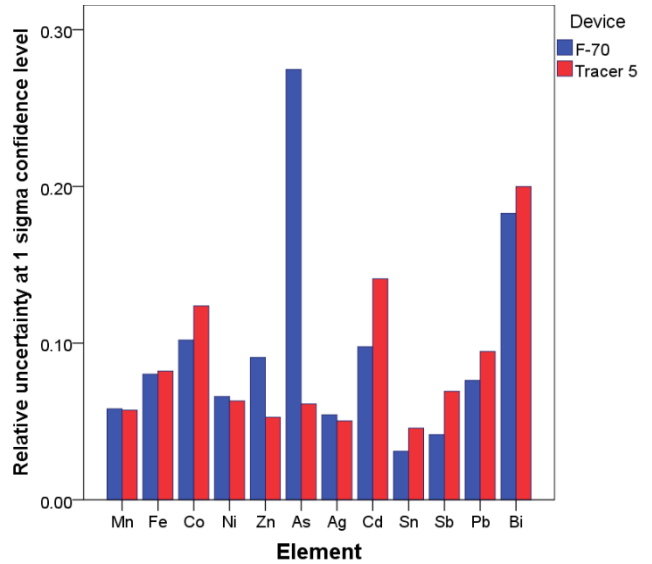


Figure 10. RUOQs at 1σ confidence level for the analysed elements. It is calculated as the standard deviation of the regression relative residuals.

$$\sigma(LOQ) = \sqrt{\left(\frac{10\sqrt{B}}{P}\sigma(c)\right)^2 + \left(\frac{5c}{P\sqrt{B}}\sigma(B)\right)^2 + \left(\frac{10c\sqrt{B}}{P^2}\sqrt{N+B}\right)^2}, \quad (4)$$

where N is the gross peak area.

For F-70, LOQs are controlled by the count-rate and improve for decreasing thicknesses until 72 and 48 μm of Cu, which both provide satisfactory results. We chose the former because of the better Sn performance. The results of Tracer 5g show that, strictly speaking, the lowest average LOQ is provided by 40 kV and a combination of Ti 25 μm and Al 300 μm . However, we decided to use the same filters and a higher voltage (49 kV) to ensure the best possible excitation of Sn and its neighbours.

3.2. Calibration and RUOQ

The other important use of LOQ is to establish a minimum value of c_{nom} above which a standard can be included in the calibration regression. Figure 9 compares the LOQs of the two devices calculated for all the analysed elements; uncertainties are quoted at 2σ confidence level. It is noteworthy that F-70

exhibits superior performance compared to Tracer 5g due to its higher primary intensity and longer measuring time. Should Tracer 5g measuring time be 100 s, LOQs would approximately halve. For elements that can be excited by Rh fluorescent lines, they would approximately equal those of F-70 or even be better. Conversely, they would double those of F-70 for medium-Z elements.

As discussed in Section 2.3, calibration is performed by weighted linear least squares fit. The standard deviation of the relative residuals provides an estimate of the relative uncertainty of quantification (RUOQ), a figure that can be extended with reasonable confidence to any copper-based alloy analysed in the same conditions. Figure 10 shows the RUOQs at 1- σ confidence level for each device and for all the analysed elements. There are no significant differences between F-70 and Tracer 5g: most elements are about 10 % or less. The important difference concerns the range of concentrations to which uncertainties refer. If we consider Sn, for example, uncertainties are similar (3 % relative versus 4.5 %), but F-70 retains this figure down to concentrations of 0.005 wt%, whereas for Tracer 5g the lower limit is 6 times higher (or 3 times higher, should the measuring time be 100 s). The high As uncertainty of F-70 is probably due to the underestimation of LOQ and to the consequent inclusion in the fit of highly uncertain data points.

4. CONCLUSIONS

This work is about quantitative methods used to tune and evaluate portable XRF spectrometers. The experiments were conducted on two devices: an in-house developed spectrometer, referred to as F-70, specifically designed to investigate copper-based artefacts, and a commercial hand-held device, referred to as Bruker Tracer 5g. Although the Bruker as purchased was virtually ready for use, we preferred to reconfigure it from scratch and compare its performance with the more "transparent" F-70. The paper discusses the process of optimizing the primary spectrum and calibrating the instruments to prepare them for field use. The method that we used to optimise the primary spectrum consists in placing different filters on the path of the primary beam and considering the corresponding limits of quantification, that we used as a figure of merit to evaluate excitation efficiency. Ideally, the optimum filter is the one that minimises the limits of quantification. In fact, it is a compromise solution among elements with absorption edges at different energies. The filters that we selected are 72 μm of Cu for F-70 and 25 μm of Ti plus 300 μm of Al for Tracer 5g.

We also used the limits of quantification to select the standards for the calibration regression: those with c_{nom} above the limit of quantification were included. Different from reference [9], we introduced the weights $1/c_{\text{nom}}^2$ in the regression to reduce the weight of data points with high c_{nom} and improve accuracy at low concentrations.

The standard deviation of the regression residuals was taken as an estimate of the relative quantification uncertainty (RUOQ) at 1- σ confidence level.

Comparison of the two devices shows that the limits of quantification of F-70 are significantly lower, due to the higher tube voltage and current and to a longer measuring time. They range from 0.005 % for Sn to 0.06 % for As, whereas those of

Tracer 5g range from 0.02 % for Co to 0.1 % for As. Increasing measuring time to 100 s would halve these figures. Relative uncertainties of quantification are similar, around 10 % or less. Due to lower limits of quantification, however, F-70 retains these figures down to concentrations considerably lower than those of Tracer 5g.

ACKNOWLEDGEMENT

The authors are grateful for the Erasmus+ program which supported the traineeship on analysing heritage metals using high-energy XRF spectrometry at the Institute of Heritage Science of the National Research Council in Rome.

REFERENCES

- [1] C. M. Kraay, The Composition of electrum coinage, *Archaeometry*, 1 (1958), pp. 21-23.
DOI: [10.2307/505360](https://doi.org/10.2307/505360)
- [2] R. Cesareo, F. V. Frazzoli, C. Mancini, S. Sciuti, M. Marabelli, P. Mora, P. Rotondi, G. Urbani, Non-destructive analysis of chemical elements in paintings and enamels, *Archaeometry*, 14 (1972), pp. 65-78.
DOI: [10.1111/j.1475-4754.1972.tb00051.x](https://doi.org/10.1111/j.1475-4754.1972.tb00051.x)
- [3] E. T. Hall, F. Schweizer, P. A. Toller, X-ray fluorescence analysis of museum objects: a new instrument, *Archaeometry*, 15 (1973), pp. 53-78.
DOI: [10.1111/j.1475-4754.1973.tb00076.x](https://doi.org/10.1111/j.1475-4754.1973.tb00076.x)
- [4] S. Piorek, Handheld x-ray fluorescence (HHXRF) in: *Portable Spectroscopy and Spectrometry 2: Applications*. R. Crocombe, P. Leary, B. Kammrath (editors), John Wiley and Sons Ltd, 2021, ISBN 9781119636489, pp. 423-453.
DOI: [10.1002/9781119636489.ch41](https://doi.org/10.1002/9781119636489.ch41),
- [5] M. Ferretti, The investigation of ancient metal artefacts by portable X-ray fluorescence devices, *Journal of Analytical Atomic Spectrometry*, 29 (2014), pp. 1753-1766.
DOI: [10.1039/C4JA00107A](https://doi.org/10.1039/C4JA00107A)
- [6] A. Heginbotham, J. Bassett, D. Bougarit, C. Eveleigh, L. Glinesman, D. Hook, D. Smith, R. J. Speakman, (+ 2 more authors), The copper CHARM Set: a new set of certified reference materials for the standardization of quantitative X-ray fluorescence analysis of heritage copper alloys, *Archaeometry* 57 (2015) 5, pp. 856-868.
DOI: [10.1111/arc.12117](https://doi.org/10.1111/arc.12117)
- [7] V. A. Solé, E. Papillon, M. Cotte, P. Walter, J. Susini, A multiplatform code for the analysis of energy-dispersive X-ray fluorescence spectra, *Spectrochimica Acta B*, 62 (2007), pp.63-68.
DOI: [10.1016/j.sab.2006.12.002](https://doi.org/10.1016/j.sab.2006.12.002)
- [8] E. Konstantakopoulou, A. Casanova Municchia, L. Luvidi, M. Ferretti, Comparison of different methods for evaluating quantitative XRF data in copper-based artefacts, *Condensed Matter* 9 (2024) 1.
DOI: [10.3390/condmat9010005](https://doi.org/10.3390/condmat9010005)
- [9] A. Heginbotham, V. A. Solé, Charmed PyMCA, Part I: A protocol for improved inter-laboratory reproducibility in the quantitative ED-XRF analysis of copper alloys, *Archeometry* 59 (2017) 4, pp. 714-730.
DOI: [10.1111/arc.12282](https://doi.org/10.1111/arc.12282)
- [10] L. H. Keith, W. Crummett, J. Deegan, R. A. Libby, J. K. Taylor, G. Wentler, Principles of environmental analysis, *Analytical Chemistry* 55 (1983) 14, pp. 2210-2218.
DOI: [10.1021/ac00264a003](https://doi.org/10.1021/ac00264a003)